

~~CONFIDENTIAL~~

Copy 6  
RM L53F16a

NACA RM L53F16a

AUG 19 1953

UNCLASSIFIED



# RESEARCH MEMORANDUM

LOW-SPEED INVESTIGATION OF THE LATERAL CONTROL

CHARACTERISTICS OF THREE TIP AILERONS

ON A 60° TRIANGULAR WING

By Stanley M. Gottlieb

Langley Aeronautical Laboratory

Langley Field, Va.

CLASSIFICATION CANCELLED

FOR REFERENCE

A Authority *NACA R 2788* Date *10/12/54*

B By *MDA 11/9/54* See \_\_\_\_\_

NOT TO BE TAKEN FROM THIS COPY

CLASSIFIED DOCUMENT

This material contains information affecting the National Defense of the United States within the meaning of the espionage laws, Title 18, U.S.C., Secs. 793 and 794, the transmission or revelation of which in any manner to an unauthorized person is prohibited by law.

## NATIONAL ADVISORY COMMITTEE FOR AERONAUTICS

WASHINGTON

August 17, 1953

UNCLASSIFIED

~~CONFIDENTIAL~~

NACA LIBRARY

LANGLEY AERONAUTICAL LABORATORY

Langley Field, Va.

## NATIONAL ADVISORY COMMITTEE FOR AERONAUTICS

## RESEARCH MEMORANDUM

## LOW-SPEED INVESTIGATION OF THE LATERAL CONTROL

## CHARACTERISTICS OF THREE TIPAILERONS

## ON A 60° TRIANGULAR WING

By Stanley M. Gottlieb

## SUMMARY

Lateral control characteristics were obtained for three tip ailerons on a 6-percent-thick, 60° triangular-wing-fuselage combination in the Langley low-turbulence pressure tunnel at a Mach number of 0.15 and a Reynolds number of  $9 \times 10^6$ . The controls consisted of two half-delta ailerons having areas equal to 0.077 and 0.138 times the wing-semispan area and a full-delta aileron having an area equal to 0.138 times the wing-semispan area.

Calculations indicated that, in a steady roll, the large half-delta aileron was more effective than either the small half-delta or the full-delta aileron at low angles of attack. At high angles of attack, however, the full-delta aileron was the most effective. Both half-delta ailerons were underbalanced at low angles of attack and became overbalanced as the angle of attack was increased, whereas the full-delta aileron experienced the reverse trend. These changes in balance for the full-delta aileron were due to large changes in the variation of hinge-moment coefficient with angle of attack  $C_{h\alpha}$ , whereas the changes in balance for the half-delta ailerons were due to changes in both  $C_{h\alpha}$  and the variation of hinge-moment coefficient with deflection.

## INTRODUCTION

Wings of triangular plan form provide certain structural and aerodynamic characteristics that are advantageous at transonic and supersonic speeds. Numerous investigations have been made to determine the effectiveness of various types of lateral control devices on wings of this type. Data presented in references 1 and 2, for example, have shown that tip controls are more effective than flap-type controls at transonic and

supersonic speeds. At low speeds, however, data such as those presented in references 3 and 4 show that the tip controls lose their effectiveness particularly at high angles of attack. In order to determine the effectiveness as well as the hinge-moment characteristics of two different types of tip controls at low speed and high Reynolds numbers, an investigation was made in the Langley low-turbulence pressure tunnel of three tip controls on a 60° triangular-wing-fuselage combination. The controls consisted of two half-delta ailerons having areas equal to 0.077 and 0.138 times the wing-semispan area and a full-delta aileron having an area equal to 0.138 times the wing-semispan area. All tests were made at a Mach number of 0.15 and a Reynolds number of  $9 \times 10^6$ .

### SYMBOLS

Wing-fuselage forces and moments are referred to the wind axes as illustrated in figure 1.

$C_L$	lift coefficient, $\frac{\text{Lift}}{qS_w}$
$C_D$	drag coefficient, $\frac{\text{Drag}}{qS_w}$
$C_m$	pitching-moment coefficient about fuselage station 20 (fig. 1) $\frac{\text{Pitching moment}}{qS_w \bar{c}}$
$C_l$	rolling-moment coefficient, $\frac{\text{Rolling moment}}{qS_w b}$
$C_Y$	lateral-force coefficient, $\frac{\text{Lateral force}}{qS_w}$
$C_n$	yawing-moment coefficient about fuselage station 20, $\frac{\text{Yawing moment}}{qS_w b}$
$C_h$	hinge-moment coefficient, half-delta tip control, $\frac{\text{Hinge moment}}{qS_a \bar{c}_a}$

$C_h$	hinge-moment coefficient, full-delta tip control, <u>Hinge moment</u> . For aileron plan forms considered herein, $q^2 M_A$ the two definitions of hinge-moment coefficient are equivalent.
$C_{h_{tot}}$	total hinge-moment coefficient produced in steady roll for equal positive and negative deflections of ailerons on opposite wing semispans, $C_h$ (due to deflection) + $C_h$ (due to $\alpha$ )
$q$	dynamic pressure, $\rho V^2/2$ , lb/sq ft
$\rho$	air density, slugs/ cu ft
$V$	air speed, ft/sec
$S_w$	wing area, l sq ft
$S_a$	aileron area, sq ft
$b$	wing span, ft
$M_A$	moment of area of full-delta aileron about hinge line, ft <sup>3</sup>
$\bar{c}$	mean aerodynamic chord of wing, ft
$\bar{c}_a$	mean aerodynamic chord of aileron, ft
$\alpha$	angle of attack of fuselage center line, deg
$\delta_a$	deflection of aileron with respect to center line of fuse- lage, positive when trailing-edge is down, deg
$pb/2V$	wing-tip helix angle, radians
$p$	rolling velocity, radians/sec
$\left. \begin{array}{l} \Delta C_n \\ \Delta C_h \\ \Delta C_l \end{array} \right\}$	increment in coefficient due to deflection of control surface

- $C_{h\alpha}$  slope of curve of hinge-moment coefficient plotted against  $\alpha$ ,  $dC_h/d\alpha$
- $C_{h\delta}$  slope of curve of hinge-moment coefficient plotted against  $\delta$ ,  $dC_h/d\delta$

#### APPARATUS, MODEL, AND TESTS

The present investigation was conducted in the Langley low-turbulence pressure tunnel on a sting-mounted model with an electrical strain-gage balance housed within the model fuselage.

The basic model configuration had a triangular wing with  $60^\circ$  sweep-back of the leading edge, an aspect ratio of 2.31, and NACA 65A006 air-foil sections parallel to the plane of symmetry. The wing was tested in a rearward position on the fuselage (fig. 2(a)) which had a fineness ratio of 10 and whose ordinates are given in reference 5.

Two half-delta ailerons, which had areas equal to 0.077 and 0.138 times the semispan area, and a full-delta aileron, which had an area equal to 0.138 times the semispan area, were mounted on a strain-gage hinge-moment balance on the right semispan. Each of the half-delta ailerons was deflected about an axis perpendicular to the plane of symmetry, located 45 percent of the aileron root chord forward of the wing trailing edge. The full-delta aileron was deflected about the skewed parting line between the aileron and wing. For each aileron, the deflection is measured in a plane perpendicular to the hinge line. Detail dimensions of the ailerons are presented in figure 2(b). The wing, ailerons, and fuselage were constructed of steel. A photograph of the model is presented in figure 3.

The lateral control characteristics were obtained from strain-gage measurements of rolling moment, yawing moment, lateral force, and aileron hinge moment throughout an angle-of-attack range from  $-12^\circ$  to  $20^\circ$ . The data were obtained at a Reynolds number of approximately  $9 \times 10^6$  and a Mach number of approximately 0.15.

#### CORRECTIONS

The model force and moment coefficients were corrected for tunnel blocking effects by a method based on information presented in references 6 and 7. Corrections to angles of attack and drag coefficients to account for the induced upwash produced by the jet boundaries have been applied as

determined by the method of reference 8. The maximum change in aileron deflection resulting from the air loads (which occurred at  $\delta_a = 20^\circ$  for the highest angles of attack) was approximately  $0.6^\circ$ . No corrections have been applied for changes in deflection.

## RESULTS AND DISCUSSION

Lift, drag, and pitching-moment data for the basic wing-fuselage combination are presented in figure 4. Rolling-moment, hinge-moment, yawing-moment, and lateral-force coefficients for various aileron deflections are presented as functions of angle of attack in figures 5, 6, and 7 for the three ailerons tested.

### Yawing Moments

The variations in the incremental yawing-moment coefficient  $\Delta C_n$  with aileron deflection at various angles of attack are presented in figure 8 for the three ailerons tested. The full-delta aileron showed favorable yaw throughout the angle-of-attack range except at zero angle of attack at negative deflections. The half-delta ailerons, however, have unfavorable yaw at all angles of attack through the positive deflection range and at high angles of attack for negative deflections but showed favorable yaw at low angles of attack and negative deflections.

### Aileron Effectiveness

Cross plots of the increment in rolling-moment coefficient  $\Delta C_l$  against control deflection, figure 9, indicate that at all positive angles of attack for negative deflection and at angles of attack to  $10^\circ$  for positive deflections, the large half-delta aileron is the most effective and the effectiveness of the small half-delta aileron and the full-delta aileron are approximately equal. At an angle of attack above approximately  $8^\circ$ , however, both half-delta ailerons begin to lose effectiveness for positive deflections (figs. 5(a) and 6(a)) and the full-delta aileron becomes more effective (fig. 9) than either of the half-delta ailerons between angles of attack of  $10^\circ$  and  $15^\circ$ . At an angle of attack of  $15^\circ$  and positive control deflection, the maximum effectiveness of the half-delta ailerons which occurs at approximately  $12^\circ$  deflection, is equal to only one-quarter of the effectiveness of the full-delta aileron at a deflection of  $20^\circ$ . The full-delta aileron loses effectiveness at positive deflection above an angle of attack of  $16^\circ$  (fig. 7(a)), but still remains more effective than either of the half-delta ailerons. The half-delta ailerons show zero effectiveness or an actual reversal in rolling moments at an angle of attack of  $20^\circ$  for positive deflections. It should

be noted in connection with this discussion that the deflections of the half-delta and the full-delta ailerons in the stream direction are not the same because of the different orientations of the hinge lines.

For angles of attack above  $20^\circ$  the variations of rolling-moment coefficient with both angle of attack and deflection for all three ailerons are very irregular, (figs. 5(a), 6(a), 7(a)) apparently as a result of the unsteady stalled flow over the outboard regions of the wing. The inconsistent behavior of the rolling moments at high angles of attack is emphasized by the comparison of the rolling-moment coefficients for the three undeflected ailerons. At high angles of attack, two of the ailerons show large positive changes in the rolling-moment coefficient, whereas the other shows a large negative change in rolling-moment coefficient.

### Hinge Moments

The half-delta ailerons show very irregular variations of hinge-moment coefficient with angle of attack (figs. 5(a) and 6(a)). In general, zero or positive values of  $C_{h\alpha}$  are obtained through the low angle-of-attack range and larger negative values of  $C_{h\alpha}$  are obtained in the high angle-of-attack range. Although the variation of hinge-moment coefficient with angle of attack is more regular for the full-delta aileron (fig. 7(a)), large changes in  $C_{h\alpha}$  with angle of attack also occur for this aileron,  $C_{h\alpha}$  having large negative values through the low angle-of-attack range and small values at angles of attack above about  $10^\circ$ .

The variation in the incremental hinge-moment coefficient  $\Delta C_h$  with aileron deflection (fig. 10) is approximately linear for the full-delta aileron through an angle of attack of  $15^\circ$ . As the angle of attack is increased from  $0^\circ$  to  $15^\circ$ ,  $C_{h\delta}$  decreases negatively from a value of  $-0.01$  to a value of  $-0.005$ . The hinge-moment coefficients due to deflection, figure 10, of the small and large half-delta ailerons are closely balanced at low angles of attack, having values of  $C_{h\delta}$  at zero angle of attack of  $-0.0018$  and  $-0.0011$ , respectively. As the angle of attack is increased, however, the variation of hinge-moment coefficient with deflection tends to become overbalanced ( $C_{h\delta}$  positive) at low deflections.

### Characteristics in a Steady Roll

In order to make a comparison of the control characteristics in a steady roll for the three ailerons tested, values were computed for the wing-tip helix angle  $pb/2V$  and for the combined hinge moments of ailerons on both semispans of the wing deflected to equal and opposite angles.

Values of  $pb/2V$  were computed with the use of average values of damping-in-roll coefficients presented in figure 6 of reference 9. For the calculation of the total hinge-moment coefficient, the spanwise distance from the plane of symmetry used to determine the change in effective angle of attack due to rolling velocity was assumed to be the distance to the centroid of the ailerons. It should be noted that these data for total hinge-moment coefficients, which are presented in figure 11, do not show a direct comparison of the control forces for the three ailerons because of the differences in aileron dimensions.

The effectiveness of the ailerons at low angles of attack for equal up and down deflections as indicated by the values of  $pb/2V$  (fig. 11), are qualitatively affected by the changes in aileron plan form and area in the same manner as that indicated previously in the discussion of rolling-moment coefficients. At  $\alpha = 20^\circ$ , the rolling effectiveness for combined up and down deflections as indicated in figure 11 was greatest for the full-delta aileron, whereas the rolling-moment coefficients, figure 9, indicated that at positive deflections the greatest effectiveness was obtained with the full-delta aileron but at negative deflections the greatest effectiveness was obtained with the large half-delta aileron.

For all the ailerons tested, large changes in the variation of total hinge-moment coefficient with  $pb/2V$  occur with changes in angle of attack. Both half-delta ailerons were underbalanced at low angles of attack and became overbalanced as the angle of attack was increased, whereas the full-delta aileron experienced the reverse trend. Although the full-delta aileron had no physical balance and therefore a large negative variation of  $C_h$  with  $\delta$  (underbalance) as shown in figure 10, the overbalance at low angles of attack in a steady roll, shown in figure 11, is due to the large negative values of  $C_{h\alpha}$  presented in figure 7. The large decrease in the negative value of  $C_{h\alpha}$  with increase in angle of attack (fig. 7) caused a decrease in the balancing effect of the rolling velocity resulting in an underbalanced control at the high angles of attack. For the half-delta ailerons, on the other hand, a positive change in the value of  $C_{h\delta}$  in addition to the change in  $C_{h\alpha}$  (figs. 5 and 6) from a zero or positive value at low angles of attack to a negative value at high angles of attack resulted in an overbalanced condition for these controls at high angles of attack.

It should be noted that the data of figures 5, 6, and 7 indicate large irregularities at high angles of attack of the variations of rolling-moment and hinge-moment coefficient with angle of attack and deflection. It is believed, however, that the data are sufficiently systematic to indicate reliable trends of aileron balance and overbalance (fig. 11), although the magnitude of the hinge-moment coefficients indicated in figure 11 for both half-delta ailerons at high angles of attack may be questionable.

## CONCLUDING REMARKS

Calculations indicated that, in a steady roll, at low angles of attack the large half-delta aileron, which had an area equal to 0.138 times the wing-semispan area, was more effective than either the half-delta aileron having an area equal to 0.077 times the wing-semispan area or the full-delta aileron having an area equal to 0.138 times the wing-semispan area. At high angles of attack, however, the full-delta aileron was the most effective. Both half-delta ailerons were underbalanced at low angles of attack and became overbalanced as the angle of attack was increased, whereas the full-delta aileron experienced the reverse trend. These changes in balance for the full-delta aileron were due to large changes in the variation of hinge-moment coefficient with angle of attack  $C_{h\alpha}$ , whereas the changes in balance for the half-delta ailerons were due to changes in both  $C_{h\alpha}$  and the variation of hinge-moment coefficient with deflection.

Langley Aeronautical Laboratory,  
National Advisory Committee for Aeronautics,  
Langley Field, Va., June 1, 1953.

## REFERENCES

1. Stone, David G.: Comparisons of the Effectiveness and Hinge Moments of All-Movable Delta and Flap-Type Controls on Various Wings. NACA RM L51C22, 1951.
2. Sandahl, Carl A., and Strass, H. Kurt: Comparative Tests of the Rolling Effectiveness of Constant-Chord, Full-Delta, and Half-Delta Ailerons on Delta Wings at Transonic and Supersonic Speeds. NACA RM L9J26, 1949.
3. Jaquet, Byron M., and Queijo, M. J.: Low-Speed Wind-Tunnel Investigation of Lateral Control Characteristics of a 60° Triangular-Wing Model Having Half-Delta Tip Controls. NACA RM L51I10, 1951.
4. Scallion, William I.: Low-Speed Investigation of the Aerodynamic, Control, and Hinge-Moment Characteristics of Two Types of Controls on a Delta-Wing-Fuselage Model With and Without Nacelles. NACA RM L53C18, 1953.
5. Osborne, Robert S., and Mugler, John P., Jr.: Aerodynamic Characteristics of a 45° Sweptback Wing-Fuselage Combination and the Fuselage Alone Obtained in the Langley 8-Foot Transonic Tunnel. NACA RM L52E14, 1952.
6. Herriot, John G.: Blockage Corrections for Three-Dimensional-Flow Closed-Throat Wind Tunnels, With Consideration of the Effect of Compressibility. NACA Rep. 995, 1950. (Supersedes NACA RM A7B28.)
7. Glauert, H.: Wind Tunnel Interference on Wings, Bodies and Airscrews. R. & M. No. 1566, British A.R.C., 1933.
8. Katzoff, S., and Hannah, Margery E.: Calculation of Tunnel-Induced Upwash Velocities for Swept and Yawed Wings. NACA TN 1748, 1948.
9. Wolhart, Walter D.: Wind-Tunnel Investigation at Low Speed of the Effects of Symmetrical Deflection of Half-Delta Tip Controls on the Damping in Roll and Yawing Moment Due to Rolling of a Triangular-Wing Model. NACA RM L51B09, 1951.

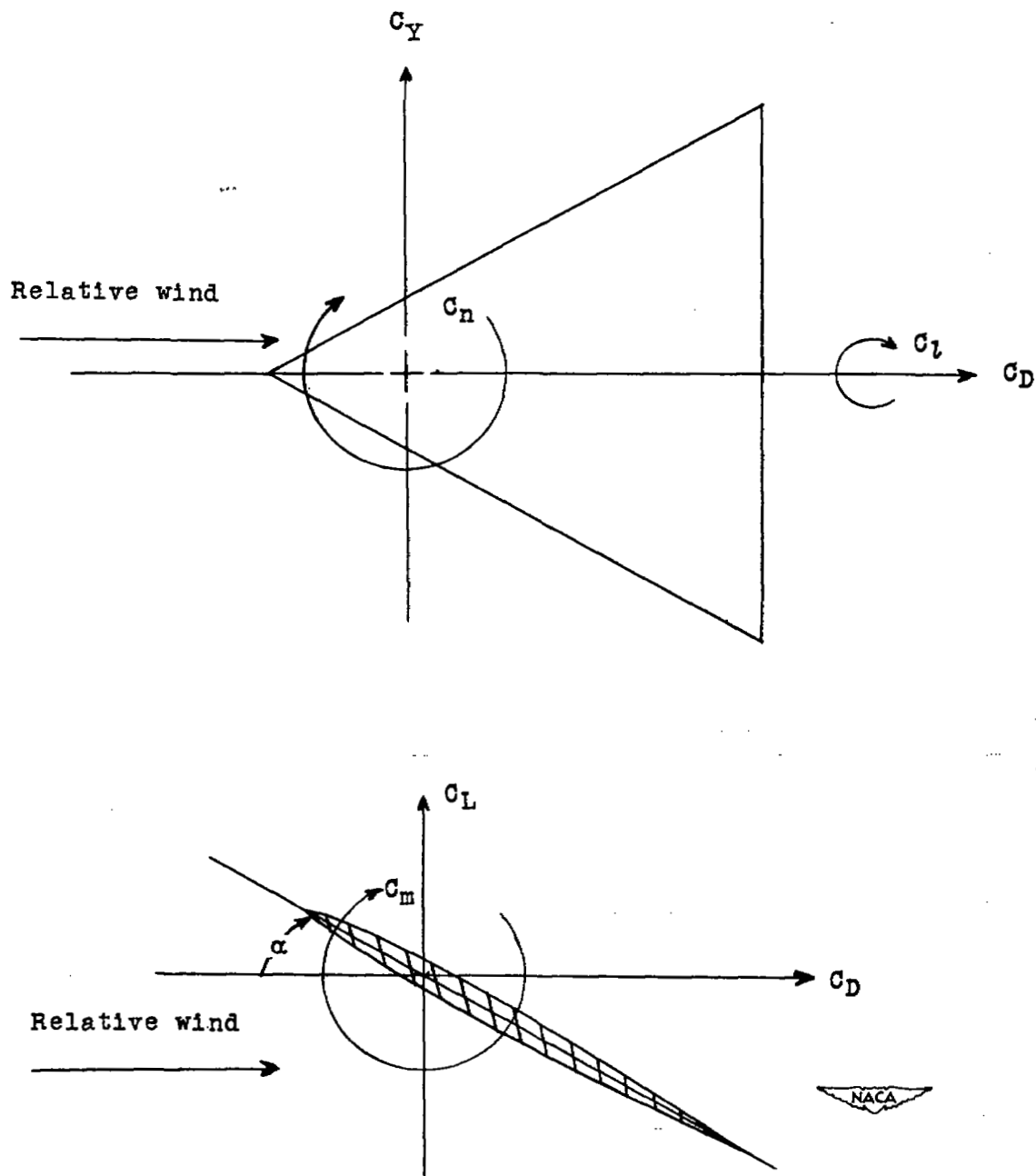
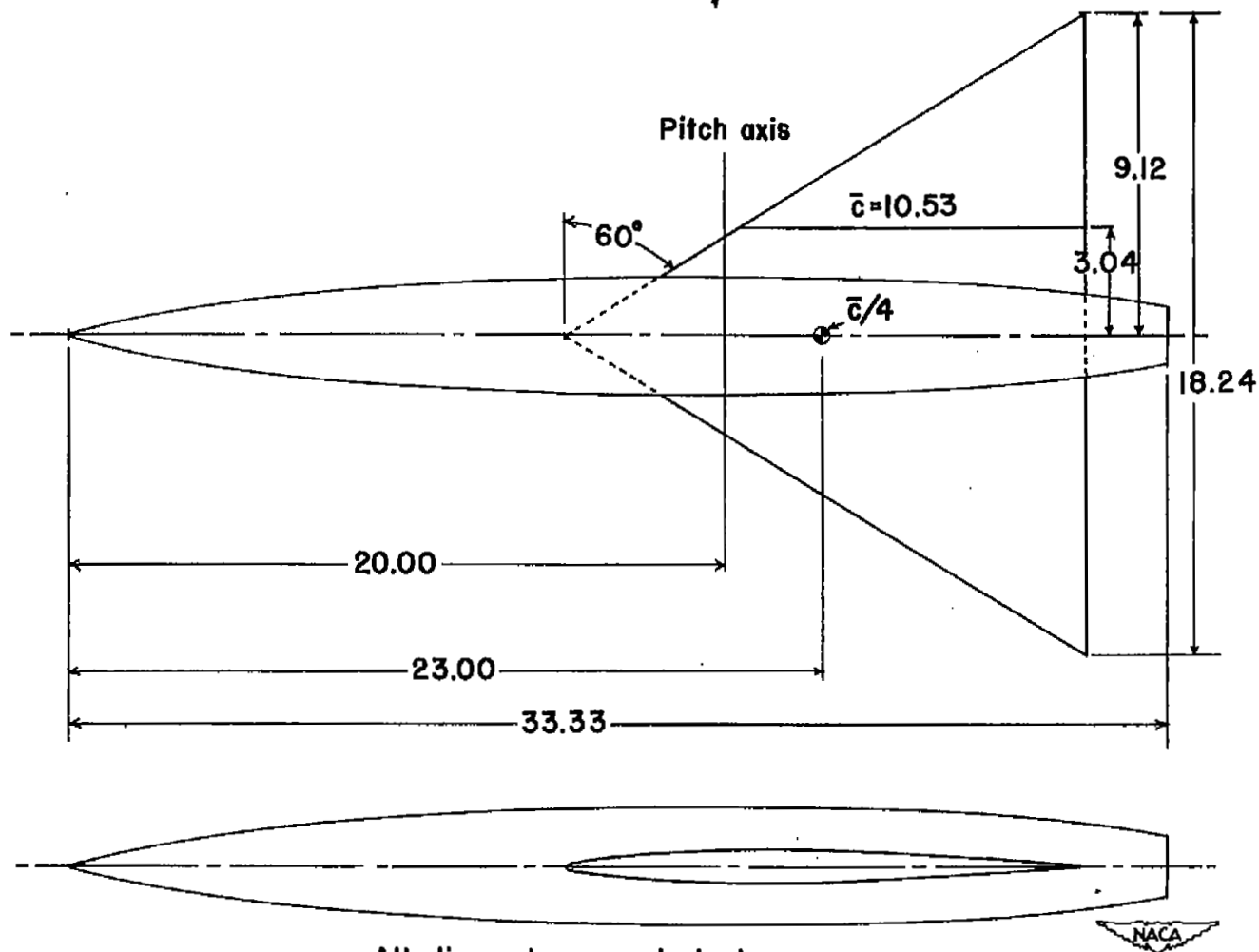


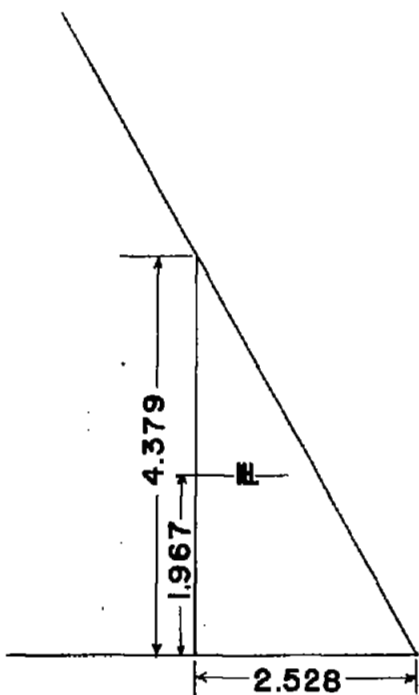
Figure 1.- System of axes used. Positive force coefficients, moment coefficients, and angles are indicated.



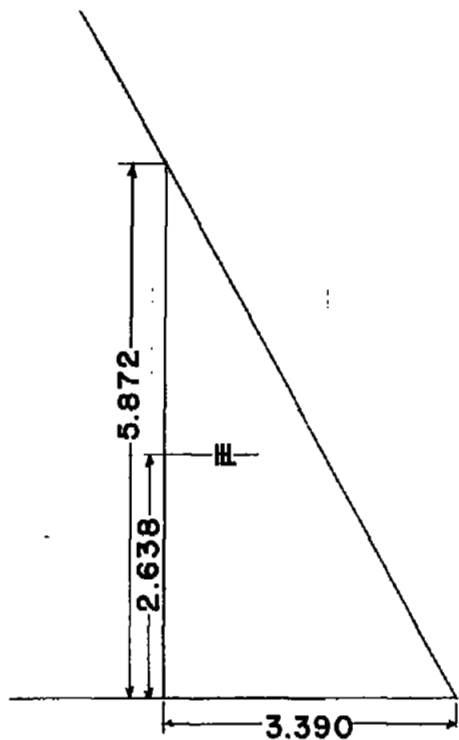
All dimensions are in inches.

(a) Basic model.

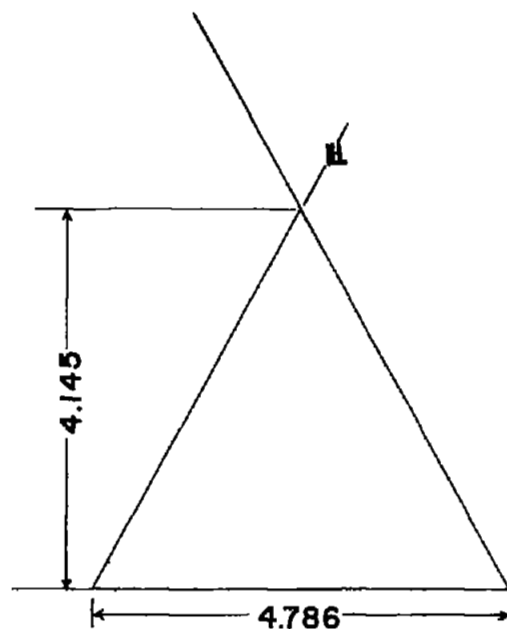
Figure 2.- Sketch of model.



Half delta,  $\frac{S_d}{S_w/2} = 0.077$



Half delta,  $\frac{S_d}{S_w/2} = 0.138$



Full delta,  $\frac{S_d}{S_w/2} = 0.138$



All dimensions are in inches.

(b) Aileron configurations.

Figure 2.- Concluded.

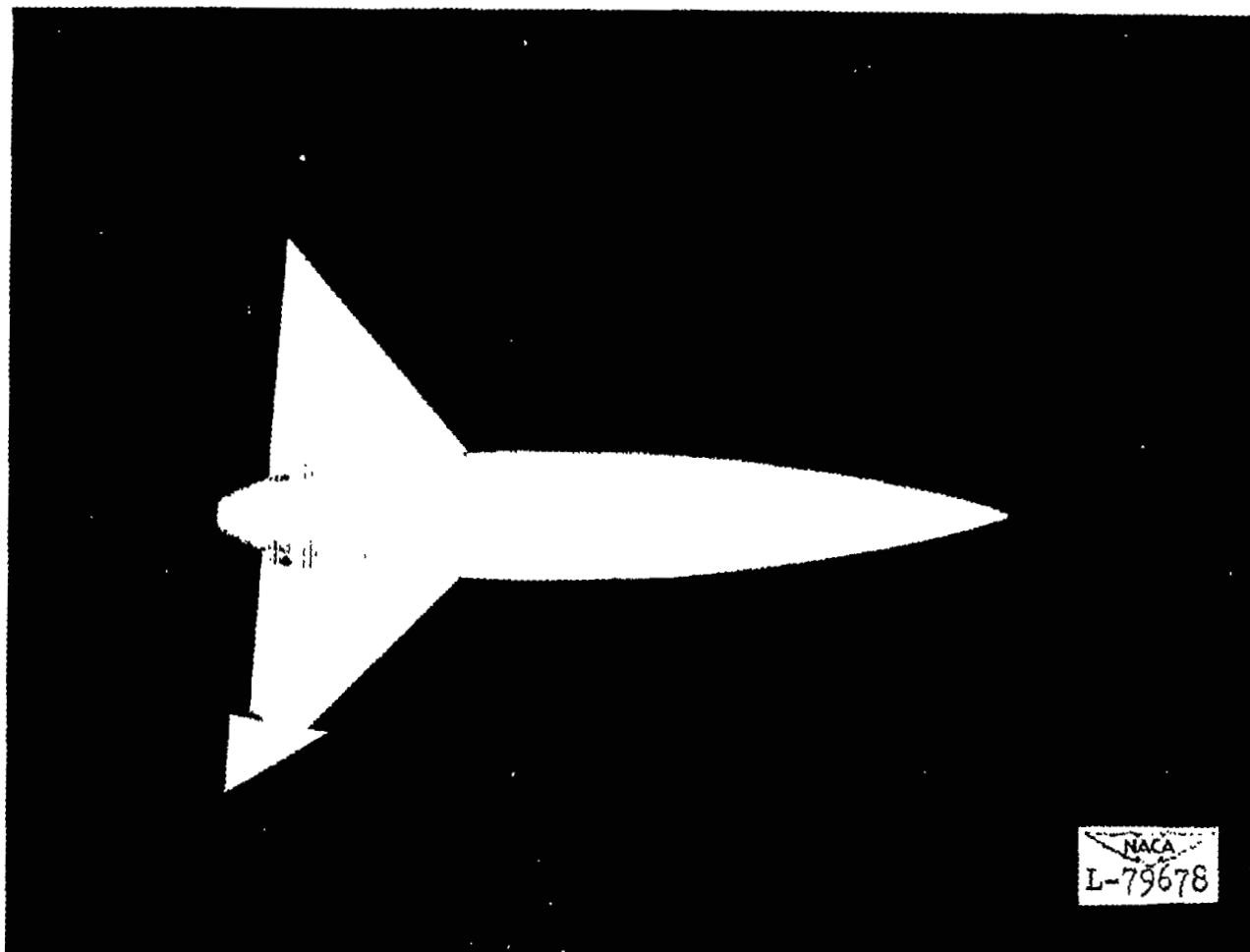


Figure 3.- Photograph of a 60° triangular-wing-body combination with a

half-delta aileron.  $\frac{S_a}{S_w/2} = 0.077$ .

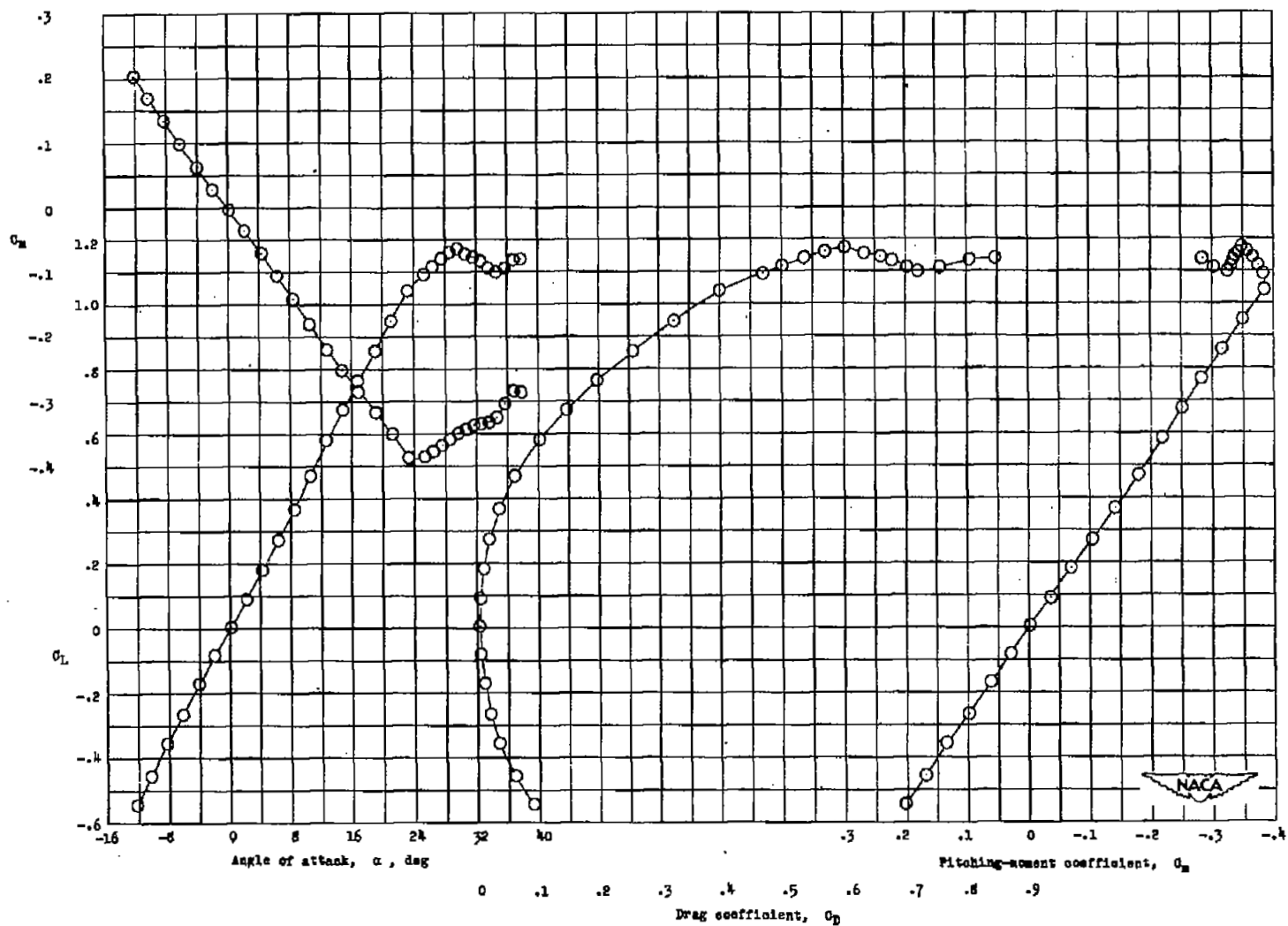
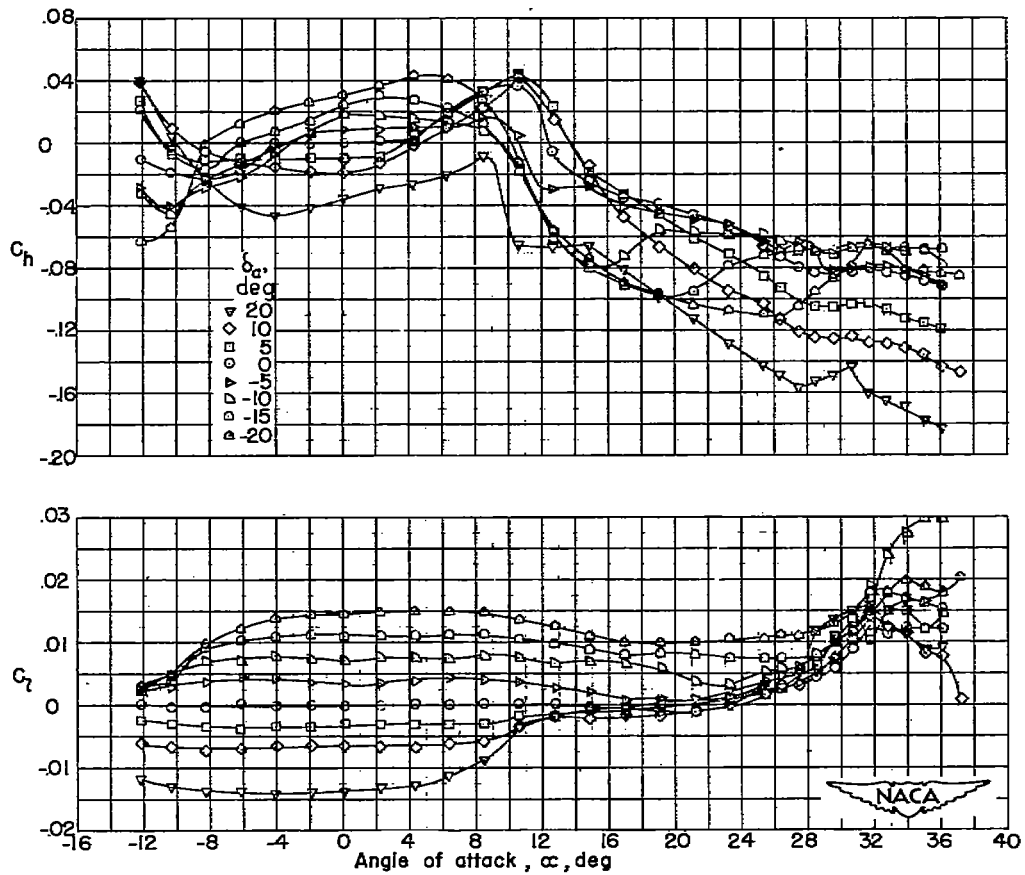


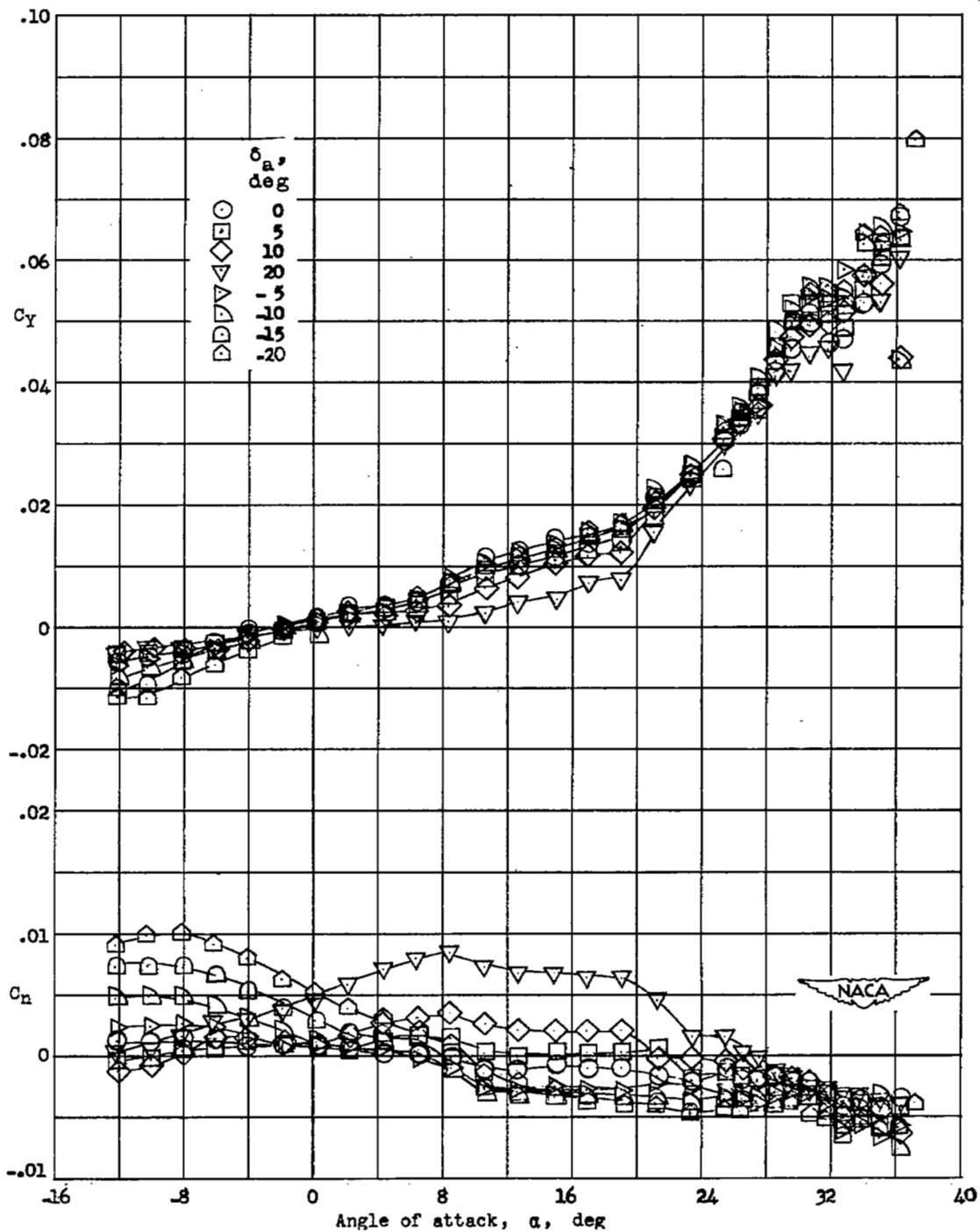
Figure 4.- Aerodynamic characteristics in pitch of a 60° triangular-wing-fuselage combination having NACA 65A006 airfoil sections.  $R = 9.0 \times 10^6$ .



(a) Effect of deflection on rolling-moment and hinge-moment coefficients.

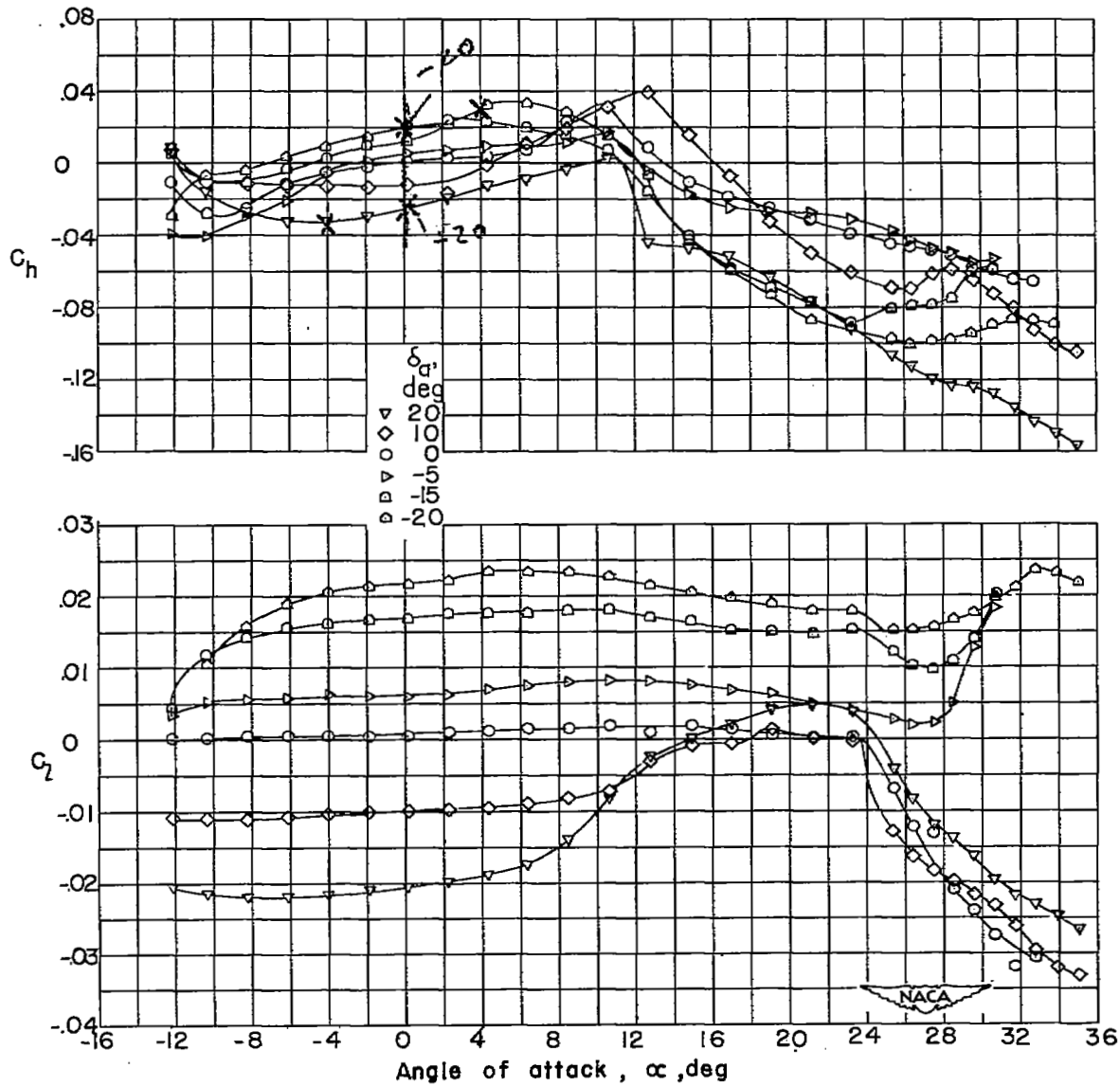
Figure 5.- Lateral control characteristics of model with half-delta aileron.

$$\frac{S_a}{S_w/2} = 0.077.$$



(b) Effect of deflection on lateral-force and yawing-moment coefficients.

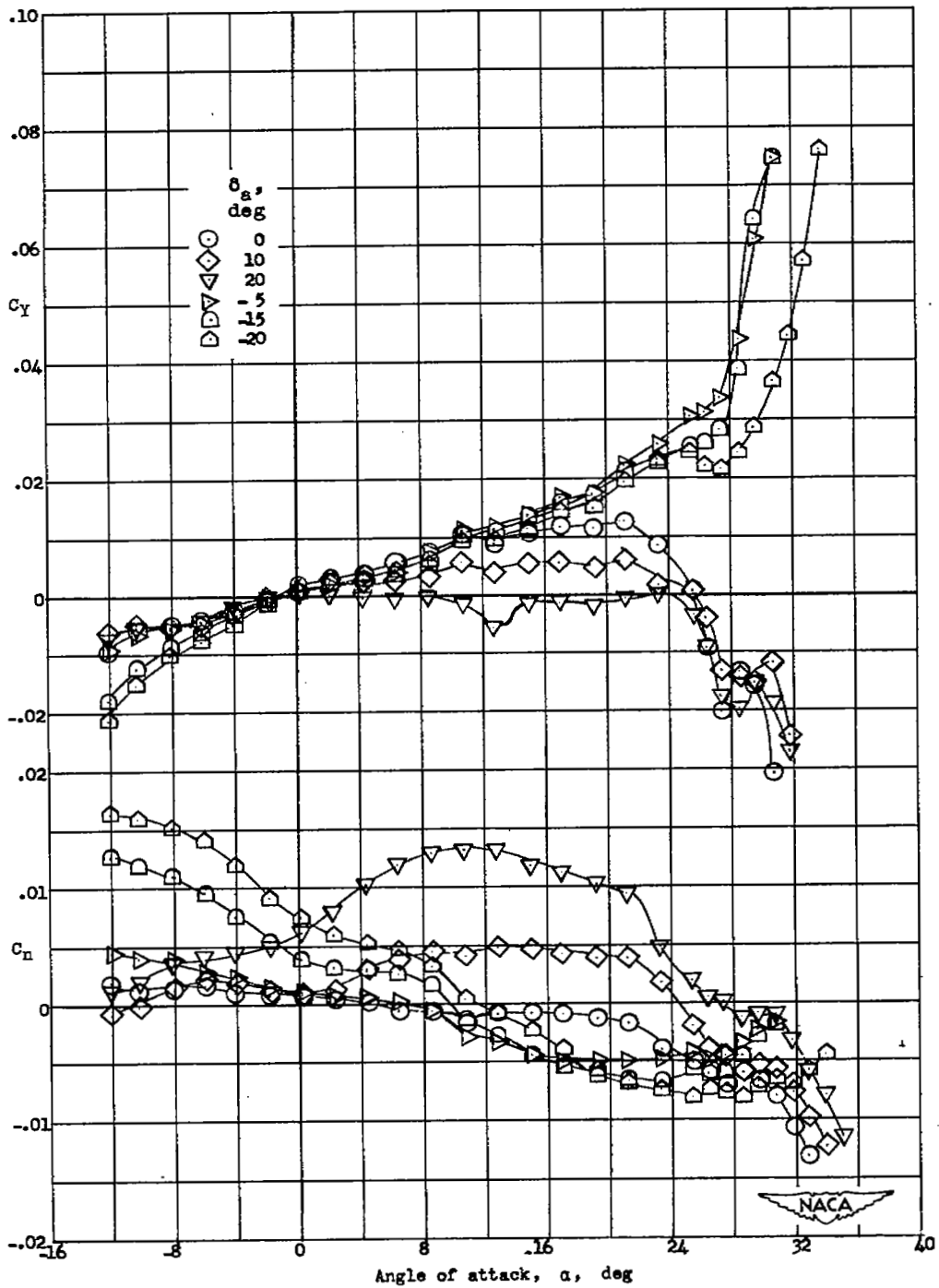
Figure 5.- Concluded.



(a) Effect of deflection on rolling-moment and hinge-moment coefficients.

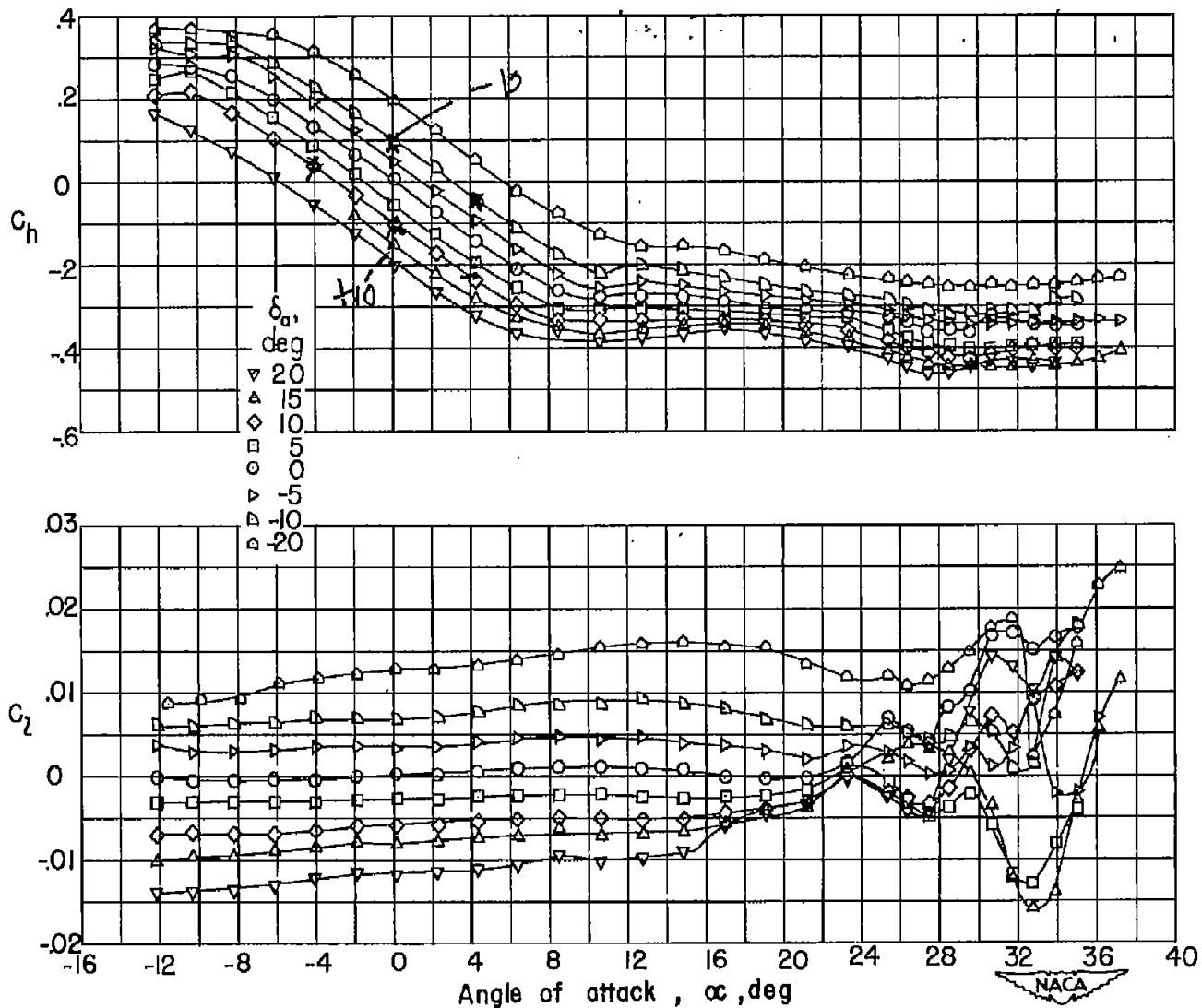
Figure 6.- Lateral control characteristics of model with half-delta aileron.

$$\frac{S_a}{S_w/2} = 0.138.$$



(b) Effect of deflection on lateral-force and yawing-moment coefficients.

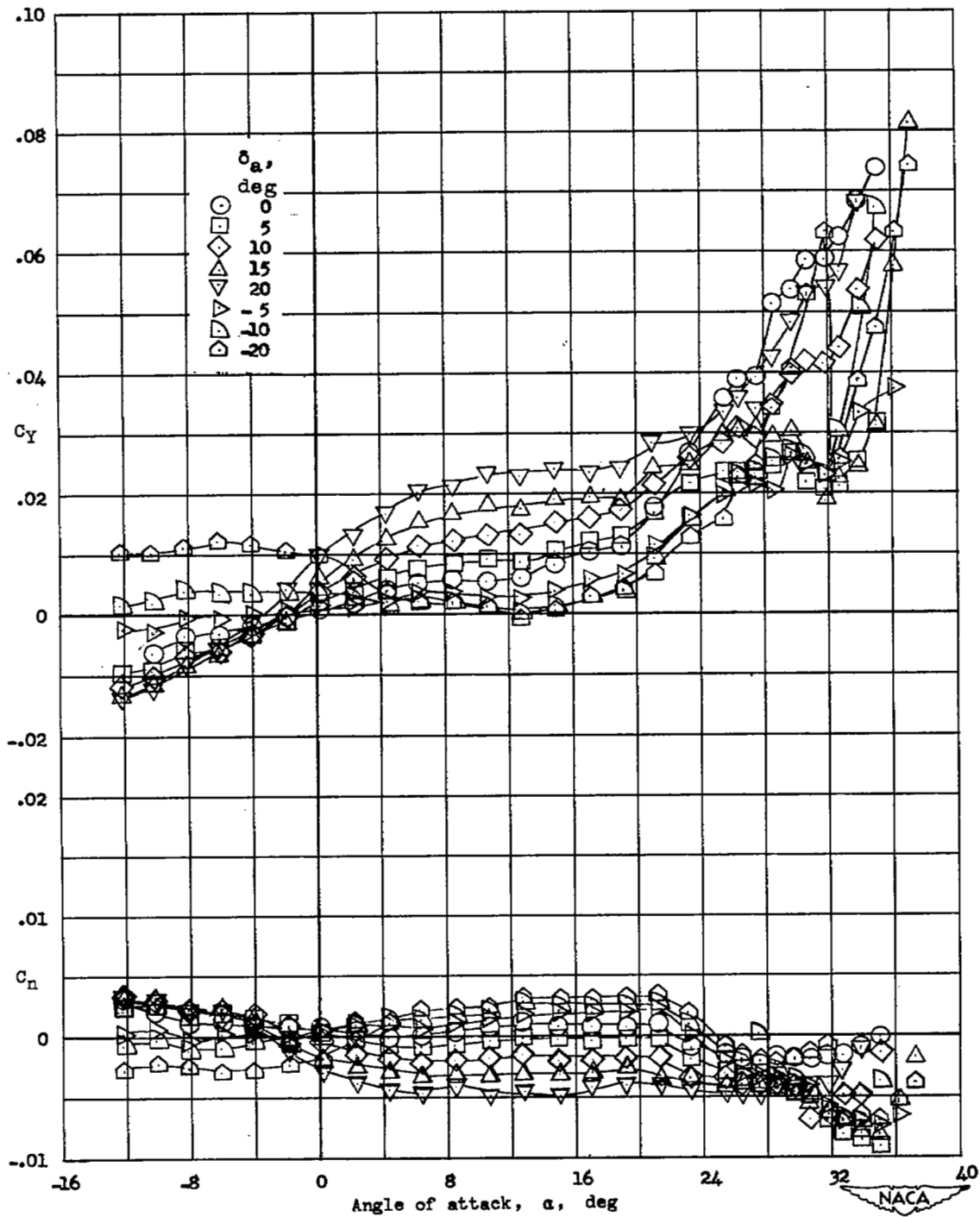
Figure 6.- Concluded.



(a) Effect of deflection on rolling-moment and hinge-moment coefficients.

Figure 7.- Lateral control characteristics of model with full-delta aileron.

$$\frac{S_a}{S} = 0.138.$$



(b) Effect of deflection on lateral-force and yawing-moment coefficients.

Figure 7.- Concluded.

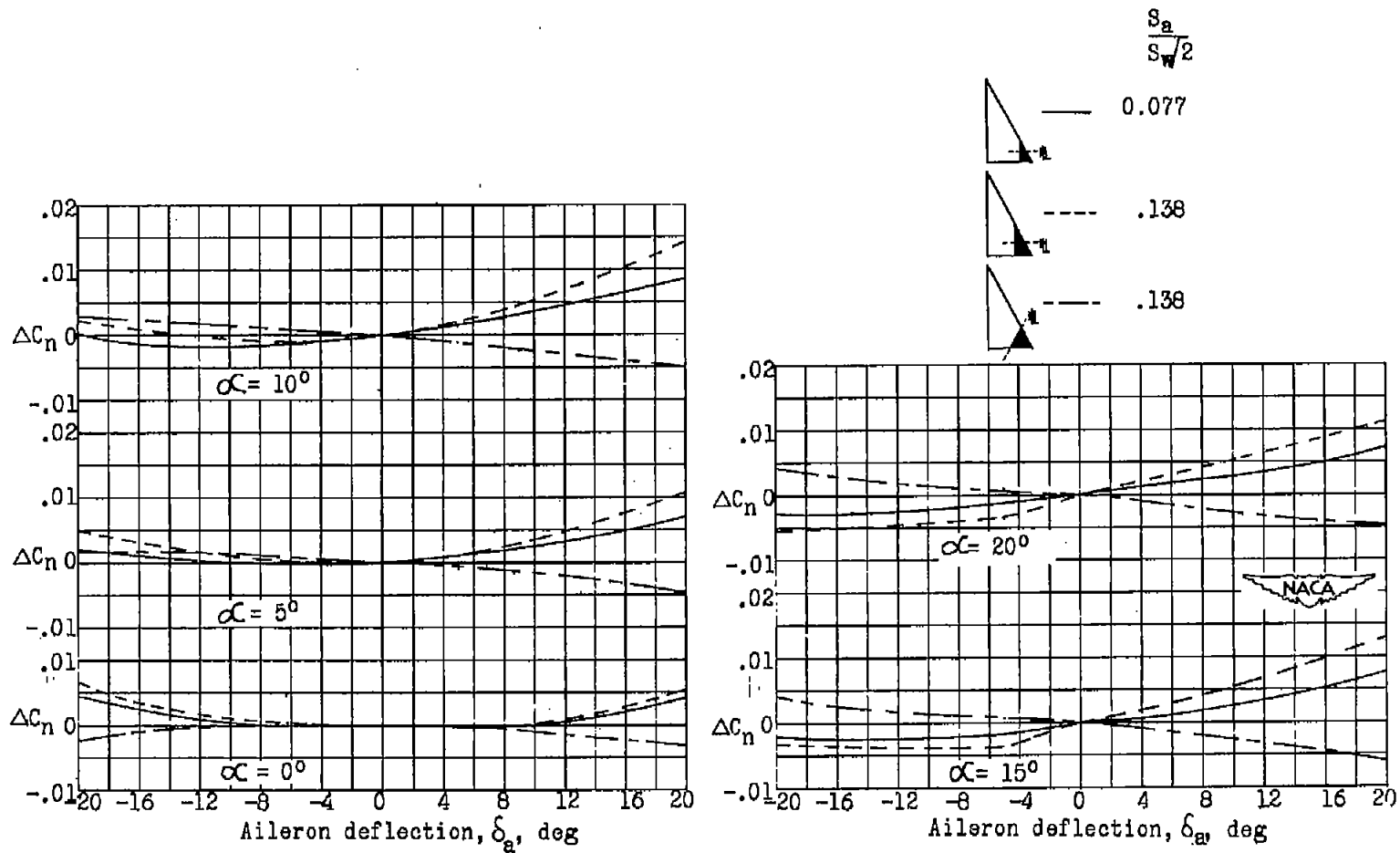


Figure 8.- Variation of increment in yawing-moment coefficient with aileron deflection for various angles of attack.

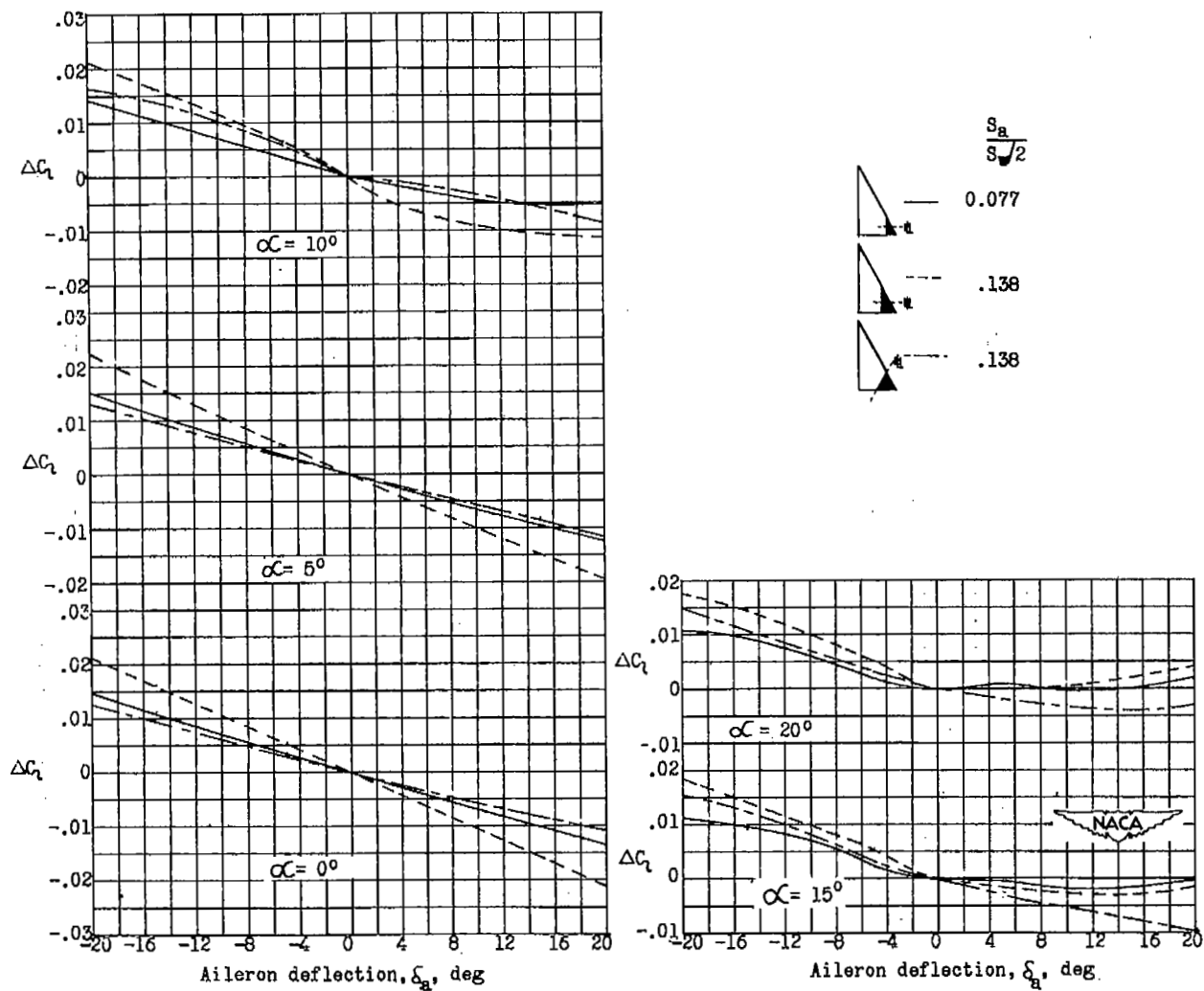


Figure 9.- Variation of increment in rolling-moment coefficient with aileron deflection for various angles of attack.

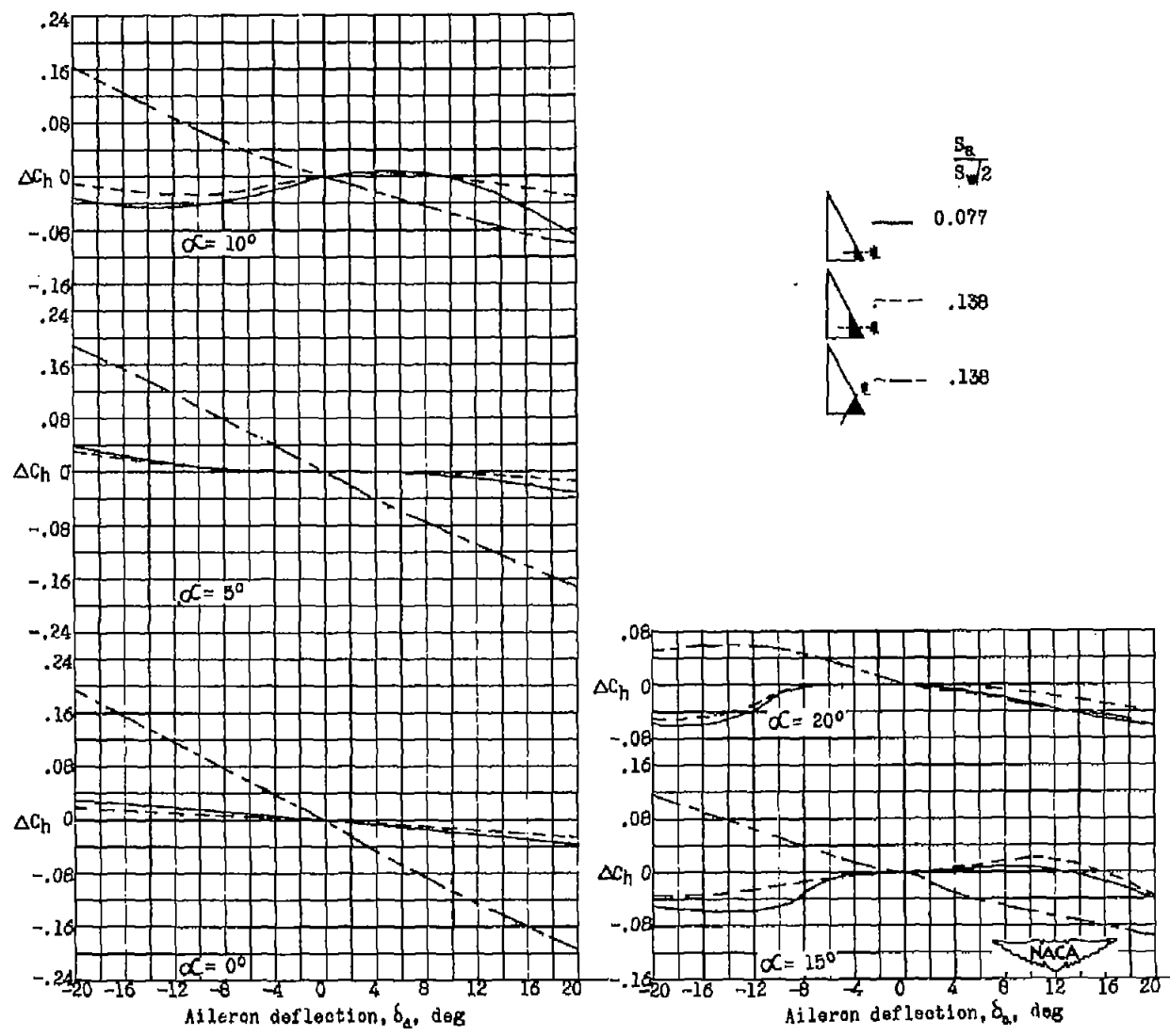


Figure 10.- Variation of increment in hinge-moment coefficient with aileron deflection for various angles of attack.

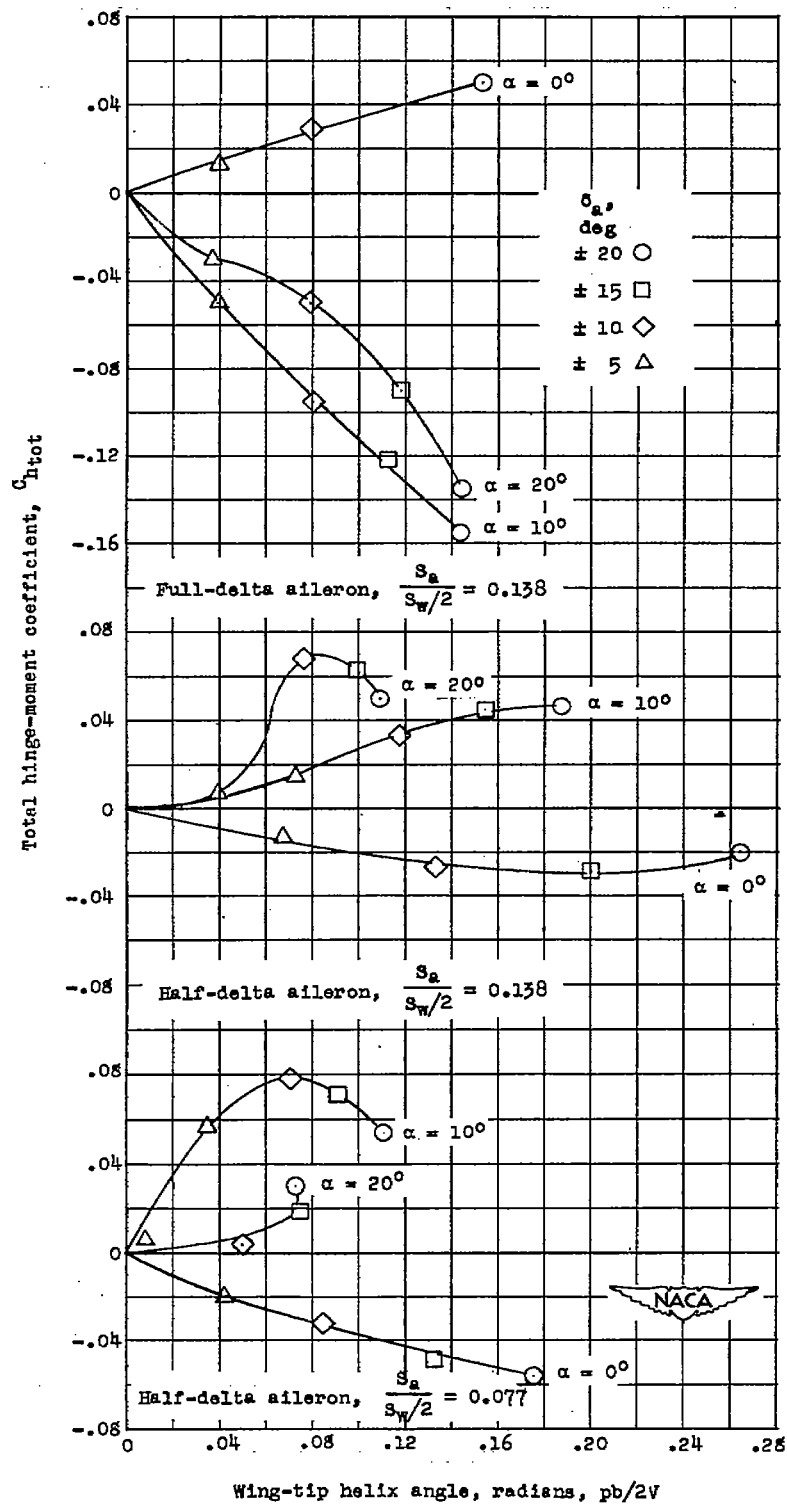


Figure 11.- Characteristics in steady roll.

SECURITY INFORMATION

~~CONFIDENTIAL~~



3 1176 01437 1166

~~CONFIDENTIAL~~